

# Comparison of Material Models for Spring Back Prediction in an Automotive Panel Using Finite Element Method

Xiongqi Peng, Shaoqing Shi, and Kangkang Hu

(Submitted May 23, 2012; in revised form October 17, 2012; published online May 29, 2013)

Springback is a crucial factor in sheet metal forming process. An accurate prediction of springback is the premise for its control. An elasto-plastic constitutive model that can fully reflect anisotropic character of sheet metal has a crucial influence in the forming simulation. The forming process simulation and springback prediction of an automobile body panel is implemented by using JSTAMP/LS-DYNA with the Yoshida-Uemori, the 3-parameter Barlat and transversely anisotropic elasto-plastic model, respectively. Simulation predictions on springback from the three constitutive models are compared with experiment measurements to demonstrate the effectiveness and accuracy of the Yoshida-Uemori model in characterizing the anisotropic material behavior of sheet metal during forming. With an accurate prediction of springback, it can provide design guideline for the practical application in mold design with springback compensation and to achieve an accurate forming.

**Keywords** forming, FEM, springback, Yoshida-Uemori Model

## 1. Introduction

Sheet metal forming is widely used in the automotive industry. Nearly 80% auto components are made by stamping. Sheet metal forming technology directly influences automobile manufacturing cost and development cycle of new cars. Involving various complex physical phenomena such as contact-impact, large deformation, and elasto-plasticity, it is difficult to design and control sheet metal forming process, resulting in many defects in the forming process, among which wrinkling, cracking, and springback are the three major defects. Dimension accuracy is a major concern in sheet metal forming process, due to considerable elastic recovery during unloading, which leads to springback (Ref 1). It requires an accurate prediction on springback in mold design for springback control and accurate forming (Ref 2-4).

Since NUMISHEET'93, there have been regular springback benchmarks, and many research efforts have been devoted to understanding springback mechanism for controlling it and achieving an accurate sheet metal forming, by experiment approaches (Ref 5-11), developing analytical models (Ref 1, 12-19) and using numerical simulation techniques. Springback is affected by a combination of various process parameters such as part dimension and shape, sheet thickness and material properties, type of process and lubrication

conditions, etc. These complexities limit the application of experimental approaches and analytical models in the accurate prediction of springback, which is of vital importance in the design of tools and forming process. Alternatively, the application of numerical simulation techniques, especially finite element method (FEM), and computer-aided design is becoming essential in modern metal-forming technology (Ref 20, 21).

The prediction of springback by using FEM has been carried out by many investigators in the past. Taylor et al. (Ref 22) used the combination of implicit and explicit FEM with ABAQUS to simulate benchmark problems of NUMISHEET'93. Chou and Hung (Ref 23) investigated springback reduction techniques including arc bottoming, pinching die, and spanking in U-channel bending processes. By combining optimization with FE analysis, optimum forming parameters based on springback reduction were identified. Taking a 2D U-draw bending as an example, Papeleux and Ponthot (Ref 24) investigated the effects of numerical and physical parameters on effectiveness and suitability of numerical simulation on springback. Taking into account uncertainties in material properties and process conditions in a sheet metal flanging process, Buranathiti and Cao (Ref 25) proposed model validation approaches for simulation-based models and for reducing costly physical experiments. Panthi et al. (Ref 26) analyzed springback in sheet metal bending by using an algorithm based on Total-Elastic-Incremental-Plastic Strain with large strain and rotation. The effects of sheet thickness as well as die radius on springback were investigated. By using Hill's quadratic yield function, Firat et al. (Ref 27) presented a rate-independent anisotropic plasticity model taking into account the Bauschinger effect and applied it to the springback of the Numisheet'93 U-channel benchmark. Other works including the Bauschinger effect and time-dependent properties of springback can be found in Ref 28 and 29.

The springback of sheet metal is a highly non-linear process (Ref 30). It requires delicate treatments in numerical simulations

Xiongqi Peng, and Kangkang Hu, School of Materials Science and Engineering, Shanghai Jiao Tong University, 1954 Huashan Road, Shanghai, China 20030; and Shaoqing Shi, Department of Civil Engineering, Logistical Engineering University, Chongqing 401311, China. Contact e-mail: xqpeng@sjtu.edu.cn.

including advanced computational algorithm for contact definition and convergence criteria for solutions, robust element types and especially appropriate constitutive models (Ref 31). Sheet metals usually render anisotropy and it is crucial to reflect this anisotropic material behavior appropriately for an accurate stress calculation and thus an effective springback prediction (Ref 32-34). In this paper, the forming process simulation and springback prediction of an automobile body panel made from high strength steel are implemented by using FE software package JSTAMP/LS-DYNA. Yoshida-Uemori constitutive model (Ref 35, 36) is selected to characterize the anisotropic material behavior of the high strength steel sheet during forming. Simulation predictions on springback are compared with experiment measurements along with numerical results from the 3-parameter Barlat model and transversely anisotropic elasto-plastic model to demonstrate the effectiveness and suitability of the Yoshida-Uemori model. By achieving an accurate prediction of springback, it can provide theoretical basis for the practical application in mold design for springback control and accurate forming.

## 2. Yoshida-Uemori Material Model

The Yoshida-Uemori kinematical hardening material model (Y-U model) adopts Hill's 48 anisotropic yield function which assumes consistence between the orthogonal coordinate system and the anisotropy axis:

$$\sqrt{F(\sigma_y - \sigma_z)^2 + G(\sigma_z - \sigma_x)^2 + H(\sigma_x - \sigma_y)^2 + 2L\sigma_{yz}^2 + 2M\sigma_{zx}^2 + 2N\sigma_{xy}^2} = \sigma_{0Y}(\bar{\epsilon}^P) \quad (\text{Eq 1})$$

where  $\sigma_{0Y}(\bar{\epsilon}^P)$  is the yield stress along the rolling direction.  $F, G, H, L, M, N$  are anisotropic material constants and can be calculated from the three anisotropic parameters  $R_0, R_{45},$  and  $R_{90}$  along the directions which are  $0^\circ, 45^\circ,$  and  $90^\circ$  to the rolling direction, respectively:

$$H = \frac{R_0}{1 + R_0}, \quad G = \frac{H}{R_0}, \quad F = \frac{H}{R_{90}}, \quad (\text{Eq 2})$$

$$N = (R_{45} + 1/2)(F + G), \quad L = 1.5, \quad M = 1.5$$

Young's modulus has a great influence on the prediction accuracy of springback in forming numerical simulation. In stamping process, Young's modulus varies considerably with the increase of plastic deformation. In the Y-U model, the variation of Young's modulus with respect to plastic strain is described by (Ref 35, 36)

$$E(\bar{\epsilon}^P) = E_0 - (E_0 - E_a)[1 - \exp(-\xi\bar{\epsilon}^P)] \quad (\text{Eq 3})$$

where  $E_0$  and  $E_a$  stand for Young's modulus for initial and infinitely large prestrained materials, respectively.  $\bar{\epsilon}^P$  denotes effective plastic strain.  $\xi$  is a material constant.

The Y-U model assumes that the magnitude and shape of the yield surface keep unchanged during plastic deformation. It can only translate as a whole in the stress space. As schematically shown in Fig. 1, the Y-U kinematical hardening model can be described by a yield surface  $f$  with back stress  $\alpha$  and a boundary

surface  $F$  with back stress  $\beta$ . The center of the yield surface  $f$  just moves with the back stress  $\alpha$ . The boundary surface  $F$  expands with the hardening of plastic strain and can be described by  $(B + R)$ . The back stress  $\alpha$  consists of two components  $\beta$  and  $\alpha^*$ , which are defined by

$$\begin{cases} \alpha = \beta + \alpha^* \\ \dot{\beta} = m\left(\frac{2}{3}b\dot{\epsilon}^P - \beta \cdot \dot{\epsilon}^P\right) \\ \dot{\alpha}^* = C\left[\frac{B+R-Y}{Y}(\sigma - \alpha)\dot{\epsilon}^P - \alpha^* \sqrt{\frac{a}{\sigma}}\dot{\epsilon}^P\right] \end{cases} \quad (\text{Eq 4})$$

where  $\alpha^*$  is the relative kinematic motion of the yield surface  $f$  with respect to the bounding surface  $F$ .  $m$  and  $b$  are material parameters determining anisotropy in Hills (1990) yield criterion.  $C$  is the material parameter for kinematic hardening rule of yield surface.  $B$  is the initial size of the bounding surface.  $Y$  is the initial yield strength.  $R$  is the isotropic hardening component of the bounding surface.

The expanding rate of the boundary surface  $F$  is defined by

$$\dot{R} = m(R_{\text{sat}} - R)\dot{\epsilon}^P \quad (\text{Eq 5})$$

where  $\dot{R}$  is the rate of expansion of the bounding surface.  $R_{\text{sat}}$  is the material parameter for isotropic hardening rule of the bounding surface. In the Y-U model, except for the six parameters,  $Y, C, B, m, b, R_{\text{sat}}$ , another parameter  $h$  is used to express hardening stagnation (Ref 35, 36).

The Y-U model is an elasto-plastic model with double yield surfaces. It introduces a constraint surface to make the boundary surface produce non-isotropic hardening through

the forward and reverse strain paths, thus making it be capable of describing hardening stagnation and following overall hardening. Additionally, the constraint surface of the Y-U model is defined in the deviatoric stress space and avoids the problem of being unable to define plastic strain space for the case of lager shear strain. The Y-U model overcomes the shortage of other kinematic hardening models by the

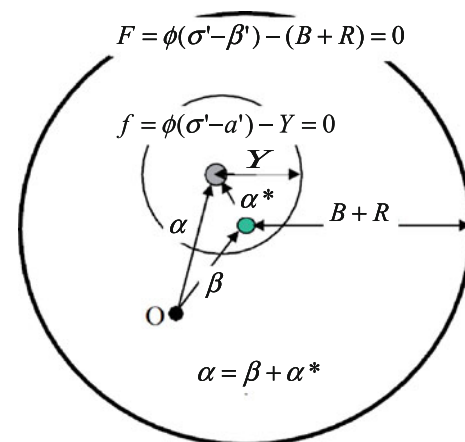


Fig. 1 Yoshida-Uemori kinematical hardening model (Ref 35, 36)

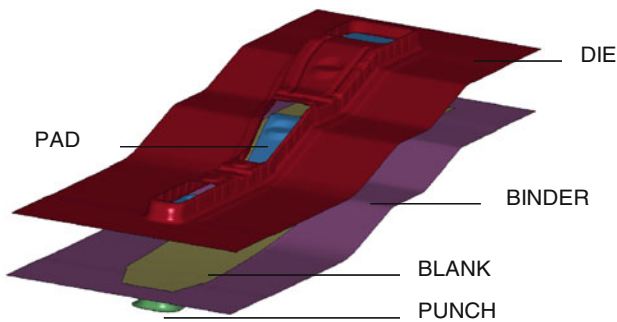


Fig. 2 FE model for forming of an automotive panel

description of hardening stagnation. By combining with Hill's 90 anisotropic yield function, Yoshida used the Y-U model to predict springback of high stress steel in stretch bending (Ref 36). Comparison with experiment results demonstrated that the Y-U model provides a better springback prediction than other traditional hardening models. JSOL Corporation developed an integrated forming simulation system named JSTAMP based on LS-DYNA, and the Y-U model is programmed as a user subroutine in LS-DYNA for springback simulation. JSTAMP established a specific material database for the Y-U model through a large number of experimental data, which improves the accuracy of springback analysis. In this paper, the forming process simulation and springback prediction of an automobile body panel made from a high strength is implemented by using JSTAMP/LS-DYNA. Both the Y-U hardening model and isotropic hardening models are used and compared to demonstrate the effectiveness and accuracy of the former.

### 3. Finite Element Model and Forming Simulation Results

Figure 2 shows the FEM model for the stamping of the automobile body panel, including punch, die, blank, binder, and pad. The minimum tooling radius is 3 mm. A binder force of 150 kN is imposed on the binder to prevent wrinkling. A force of 15 kN is imposed on the pad to prevent blank moving and bouncing during forming. An inverted drawing structure is adopted for the mold and single action is selected as its process type.

The original length and width of the blank are 1420 mm × 278 mm with a uniform thickness of 1.10 mm. The blank material is DP600 high strength steel. Its main material parameters are listed in Table 1. The forming simulation is implemented by using JSTAMP/LS-DYNA software. Penalty-based contact algorithm and "forming-one-way" contact interface type in LS-DYNA are chosen. Coulomb law is used to define contact friction. The main processing parameters are shown in Table 2. The maximum velocity of the punch in the real forming is 0.5 m/s. Various tooling speeds including 2, 5, and 10 m/s were selected in the numerical simulation for trial computation. Special attention was paid to the dynamic effects introduced by the artificial increase in tooling speed. The ratio of internal to kinetic energy in the blank was closely monitored. It was found that by setting the punch speed as 5 m/s, stable results can be obtained with good computational efficiency. Hence in the following calculation, the punch speed is set to be

Table 1 Material parameters of DP600 (thickness: 1.1 mm)

Density, kg/mm <sup>3</sup>	Initial Young's modulus, MPa	Poisson's ratio	Yield strength, MPa	Tensile strength, MPa	<i>r</i>	<i>n</i>
$7.85 \times 10^{-9}$	$2.06 \times 10^5$	0.28	390	630	0.85	0.149

Table 2 Forming processing parameters

Punch stroke, mm	Pad stroke, mm	Binder force, kN	Pad force, kN	Friction coefficient	Velocity, m/s
55	30	150	15	0.125	5

Table 3 Material parameters for Y-U model of DP600

<i>Y</i> , MPa	<i>B</i> , MPa	<i>R</i> <sub>sat</sub> , MPa	<i>b</i> , MPa	<i>C</i>	<i>m</i>	<i>h</i>
360	435	255	66	200	26	0.3
Young's modulus		$E_o = 206 \text{ GPa}, E_a = 152 \text{ GPa}, x = 61$				

5 m/s. In addition, the effect of gravity was investigated by comparing results with those of non-gravity case with Y-U model. It was found that the effect of gravity is negligible. Hence the gravity load was neglected in the following simulations.

In the numerical simulation, the mold parts are defined as rigid bodies. The blank is discretized by quadrilateral shell elements with an overall element size of 2 mm × 2 mm and has refined mesh in potential large deformation regions contacting with tooling fillet areas. A total element number of 78351 to ensure computational accuracy for forming and springback analysis. Fully integrated element formulation is selected and the number of integration points through shell thickness is set to be 7. The simulation is implemented without adaptive mesh. The material parameters of the DP600 high strength steel for the Y-U model are shown in Table 3.

Figure 3 shows the thinning ratio of the blank after forming. As can be seen in Fig. 3, the maximum thinning ratio of the formed automobile body panel is about 20% which is within the normally acceptable range of 3 to 25%. No obvious wrinkling in the forming process is found except slight material accumulation occurs near process bars.

The forming limit diagram (FLD) is shown in Fig. 4. As can be seen in Fig. 4, the major portion of the formed automobile body panel is in the safe region, which indicates that the formability of the part is good. Also there is some insufficient stretch and wrinkling near the fringe and process bars. Those defects would not affect the normal operational usage of the formed part as they are not in the functional region of the part.

Except affected by computational errors resulting from assigned material parameters, mold geometry and friction, the accuracy on springback prediction is directly relevant to the computational accuracy on the stress field. Consequently, to ensure accurate springback prediction, it is essential to precisely control each aspect of forming simulation, eliminate accumulation error and improve computational accuracy for the stress

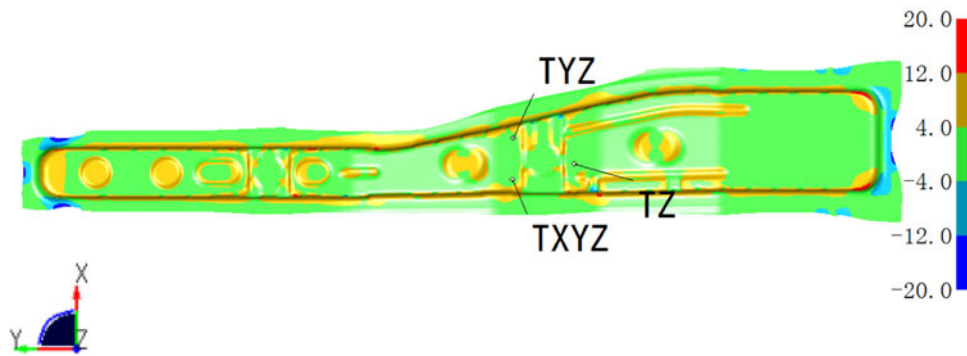


Fig. 3 Thinning distribution

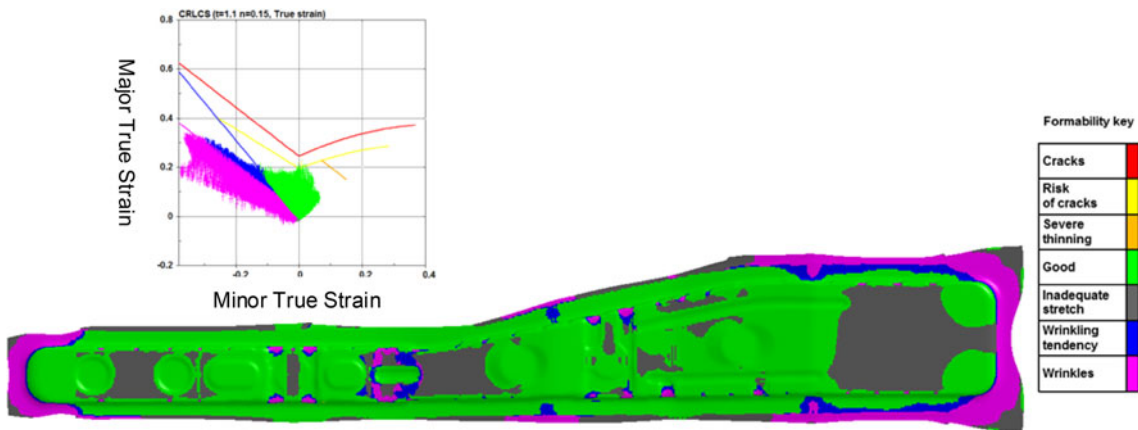


Fig. 4 Forming limit diagram

field. After forming simulation, an output file, which contains information such as nodal coordinates, strains and stresses and other simulation results, can be generated for further springback analysis. Rigid body motion should be eliminated for springback analysis. This is achieved by defining constraints on the three nodes of the blank shown in Fig. 3. The constrained nodes are picked exactly as that used in experimental measurement. The first node constrains the three translational degrees of freedom and acts as the reference point in the springback model, at which the springback displacement is set to be zero. The second node confines the global  $Y$ - and  $Z$ -translations, while the third one eliminates the global translation along the  $Z$ -direction.

Springback is actually a stress release process. There are two approaches for springback analysis: single step or multiple step springback analysis. Single step springback analysis usually leads to good results. However, converged result may not be obtained using single step analysis for relatively flexible part. Thus multiple step approach is chosen in the springback analysis in order to obtain a converged result. In this approach, the springback deformation is divided into several smaller, more manageable steps. This is accomplished by automatically inserting artificial spring constraints at each nodal point. These artificial springs resist deformation, making equilibrium easier to achieve. As the solution proceeds, these springs are automatically relaxed, until they are removed entirely at the termination time.

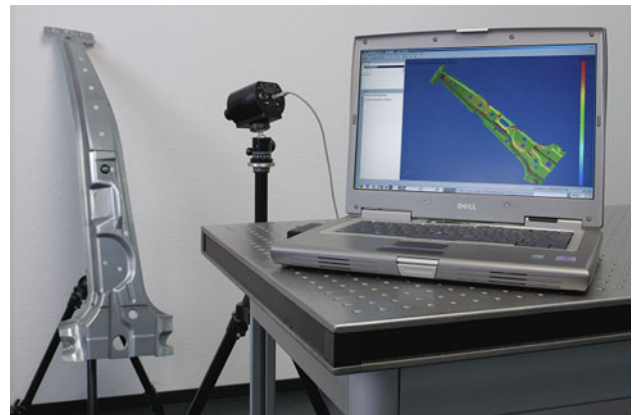


Fig. 5 Springback measurement with a GOM ATOS whitelight scanner

#### 4. Result Analysis and Discussion

Currently, there are mainly three kinds of methods to measure the amount of springback. The first one is to cut different sections of the formed part to measure the 2D deviations of the part from the corresponding mold section after springback. This method is mainly used in the springback

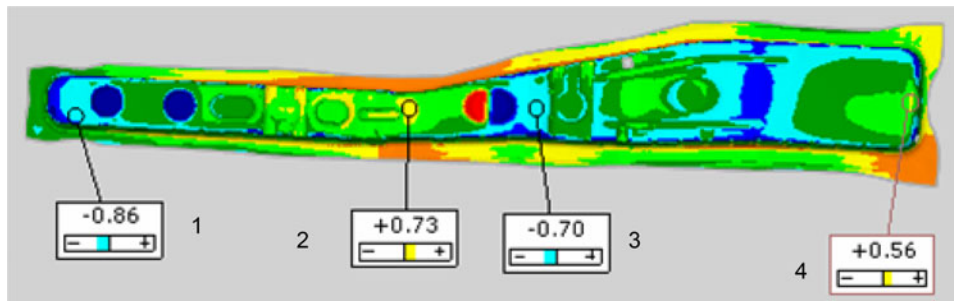


Fig. 6 Experimental result of springback

Table 4 Comparison of experimental and simulation results for springback

Comparison	Position				
	1	2	3	4	
Experimental result, mm	-0.86	0.73	-0.70	0.56	
Y-U model, mm	-0.71	0.62	-0.85	0.61	
3-Parameter Barlat model, mm	-0.56	0.30	-1.72	1.27	
Transversely anisotropic elasto-plastic model, mm	-0.51	0.63	-1.14	1.31	

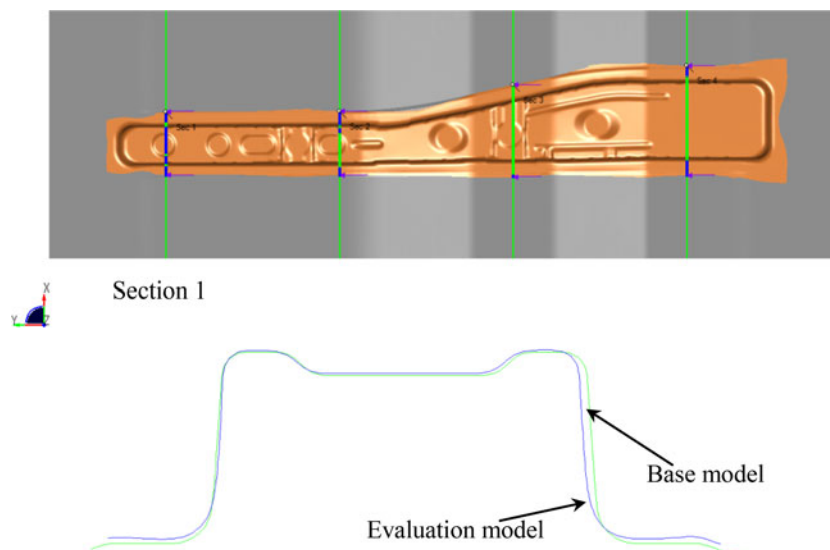


Fig. 7 Numerical springback along a section

evaluation of simple parts. The second one is to check the displacements of points on the parts after forming to characterize the springback amount. This method is currently widely used in the evaluation of springback in finite element forming simulation. The third method is to measure the deviations of the blank after springback from mold surface which is defined as the reference model. This method is suitable to evaluate the amount of springback especially for complex parts. In this paper, a GOM ATOS whitelight scanner is used for 3D digitizing and optical measurements of the formed part, as shown in Fig. 5. The positional resolution of the camera system is 800,000. The recorded 3D model data of the formed panel is compared with the CAD model of the mold surface to check the deviation of the formed part from the mold surface. Figure 6

shows the measured springback of four typical points on the panel.

In order to evaluate the accuracy of springback prediction from different hardening models, the standard LS-DYNA material models \*MAT\_3-PARAMETER\_BARLAT (MAT36) and \*MAT\_TRANSVERSELY\_ANISOTROPIC\_ELASTIC\_PLASTIC (MAT37) are used in the simulation as well. These two material models are isotropic hardening models compared with the Y-U model. Swift exponential hardening rule ( $HR = 2$ ) is chosen for the 3-parameter Barlat model with a strength coefficient  $k = 935.0$  and an exponent  $n = 0.15$ . Other specific parameters for the 3-parameter Barlat model are the exponent in Barlat's yield surface  $m = 6$ , the Lankford parameters  $R_0 = R_{45} = R_{90} = 0.85$ . The material parameters selected for

the transversely anisotropic elasto-plastic model are: Young's modulus  $E = 2.06 \times 10^5$  MPa, Poisson's ratio  $\nu = 0.28$ , the yield stress = 390 MPa, the tangent modulus  $E_t = 1.04 \times 10^3$  MPa, and the anisotropic hardening parameter  $R = 0.85$ . Stress-strain curve obtained from material testing can also be used to define the transversely anisotropic elasto-plastic model.

Numerical springback results are obtained through the geometry evaluation function of the post-processing module in JSTAMP and are then compared with experimental measurements in Fig. 6 to demonstrate the accuracy of the Y-U model. The comparison is listed in Table 4. As can be seen in Table 4, compared to the results from the 3-parameter Barlat model and the transversely anisotropic elasto-plastic model, overall, the springback predictions from the Y-U kinematic hardening model are much closer to the experiment result. The comparison demonstrates the accuracy and effectiveness of the forming simulation of the car panel using the Y-U model. By numerical simulation with the Y-U model in the virtual forming stage for springback prediction, it is feasible to make improvements for the actual production by reducing or avoiding mold trial, thus to optimize the forming process.

For complicated parts, springback varies with positions. In order to obtain an overall springback of a part, a series of section lines at different positions of the part can be picked to analyze springback comprehensively. The deviation of a section line in an evaluation model (analysis results, etc.) from the regular shape of a base model (3D data, such as CAD model or cloud data) can be checked to evaluate springback along the section. Figure 7 shows the profile of a section of the formed auto-body panel by using the Y-U model. It is compared with the corresponding section on the mold to show springback.

The preceding results indicate that the Y-U model which incorporates with Hill's 48 yield function can well predict the stress-strain response and springback of the High Strength Steel in forming. However, computationally, the Y-U kinematic hardening model is very time consuming and needs expensive memory. For some materials, especially medium strength steels, the kinematic hardening model would not be suited. Instead, classical isotropic hardening models would be more appropriate for stress-strain analysis of proportional loading cases and are more computationally economic and efficient. In springback prediction of sheet metal forming, which model to select depends on the material used as well as forming scenarios. A lot of computational exploring and extensive experience are needed for an accurate prediction.

## 5. Conclusion

The forming process simulation and springback prediction of an automobile body panel is implemented by using FE package JSTAMP/LS-DYNA. The Yoshida-Uemori constitutive model is selected to characterize the anisotropic material behavior of sheet metal during forming. Comparisons of numerical springback predictions with experiment measurements as well with numerical results from other isotropic hardening material models demonstrate the effectiveness and accuracy of the Y-U model. By using FEM and an appropriate constitutive model, accurate forming simulation and springback prediction can be achieved. Based on simulation results, it is feasible to significantly reduce the time and cost on mold trial

and modification, and thus improve forming quality of products.

## Acknowledgments

The present research is funded by China National Natural Science Foundation (50975236, 11172171).

## References

1. J. Hu, Z. Marciniak, and J. Duncan, *Mechanics of Sheet Metal Forming*, 2nd ed., Butterworth-Heinemann, Woburn, 2002
2. H. Livatyali, G.L. Kinzel, and T. Altan, Computer Aided Die Design of Straight Flanging Using Approximate Numerical Analysis, *J. Mater. Process. Technol.*, 2003, **142**, p 532–543
3. W. Gan and R.H. Wagoner, Die Design Method for Sheet Springback, *Int. J. Mech. Sci.*, 2004, **46**, p 1097–1113
4. R. Lingbeek, J. Huetink, S. Ohnimus, M. Petzoldt, and J. Weiher, The Development of a Finite Elements Based Springback Compensation Tool for Sheet Metal Products, *J. Mater. Process. Technol.*, 2005, **169**, p 115–125
5. M. Samuel, Experimental and Numerical Prediction of Springback and Side Wall Curl in U-Bending of Anisotropic Sheet Metals, *J. Mater. Process. Technol.*, 2000, **105**, p 382–393
6. V. Viswanathan, B. Kinsey, and J. Cao, Experimental Implementation of Neural Network Springback Control for Sheet Metal Forming, *J. Manuf. Sci. Eng.-Trans. ASME*, 2003, **125**, p 141–147
7. A. Andersson, Numerical and Experimental Evaluation of Springback in Advanced High Strength Steel, *J. Mater. Eng. Perform.*, 2007, **16**, p 301–307
8. K. Kuwabara, Advances in Experiments on Metal Sheets and Tubes in Support of Constitutive Modeling and Forming Simulations, *Int. J. Plast.*, 2007, **23**, p 385–419
9. U. Borah, S. Venugopal, R. Nagarajan, P.V. Sivaprasad, S. Venugopal, and B. Raj, Estimation of Springback in Double-Curvature Forming of Plates: Experimental Evaluation and Process Modeling, *Int. J. Mech. Sci.*, 2008, **50**, p 704–718
10. P. Chen, M. Koc, and M.L. Wenner, Experimental Investigation of Springback Variation in Forming of High Strength Steels, *J. Manuf. Sci. Eng.-Trans. ASME*, 2008, **130**, p 041006
11. X.J. Fu, J.J. Li, and G. Xu, Experimental Study on Springback of High Strength Sheet Metals, *Mater. Res. Innov.*, 2011, **15**, p S475–S477
12. P. Xue, T.X. Yu, and E. Chu, Theoretical Prediction of the Springback of Metal Sheets After a Double-Curvature Forming Operation, *J. Mater. Process. Technol.*, 1999, **90**, p 65–71
13. K. Anokye-Siribor and U.P. Singh, A New Analytical Model for Pressbrake Forming Using In-Process Identification of Material Characteristics, *J. Mater. Process. Technol.*, 2000, **99**, p 103–112
14. J. Chakrabarty, W.B. Lee, and K.C. Chan, An Exact Solution for the Elastic/Plastic Bending of Anisotropic Sheet Metal Under Conditions of Plane Strain, *Int. J. Mech. Sci.*, 2001, **43**, p 1871–1880
15. T. Buranathiti and J. Cao, An Effective Analytical Model for Springback Prediction in Straight Flanging Processes, *Int. J. Mater. Prod. Technol.*, 2004, **21**, p 137–153
16. B. Heller and M. Kleiner, Semi-analytical Process Modelling and Simulation of Air Bending, *J. Strain Anal. Eng.*, 2006, **41**, p 57–80
17. D.J. Zhang, Z.S. Cui, X.Y. Ruan, and Y.Q. Li, An Analytical Model for Predicting Springback and Side Wall Curl of Sheet After U-bending, *Comput. Mater. Sci.*, 2007, **38**, p 707–715
18. Y.H. Moon, D.W. Kim, and C.J. Van Tyne, Analytical Model for Prediction of Sidewall Curl During Stretch-Bend Sheet Metal Forming, *Int. J. Mech. Sci.*, 2008, **50**, p 666–675
19. H.K. Yi, D.W. Kim, C.J. Van Tyne, and Y.H. Moon, Analytical Prediction of Springback Based on Residual Differential Strain During Sheet Metal Bending, *J. Mech. Eng. Sci.*, 2008, **222**, p 117–129
20. S. Kobyashi, S. Oh, and T. Altan, *Metal Forming and the Finite Element Method*, Oxford University Press, Oxford, 1989
21. K.P. Li, W.P. Carden, and R.H. Wagoner, Simulation of Springback, *Int. J. Mech. Sci.*, 2002, **44**, p 103–122

22. L. Taylor, J. Cao, A.P. Karafillis, and M.C. Boyce, Numerical Simulations of Sheet Metal Forming, *J. Mater. Process. Technol.*, 1995, **50**, p 168–179
23. I.N. Chou and C. Hung, Finite Element Analysis and Optimization on Springback Reduction, *Int. J. Mach. Tool Manuf.*, 1999, **39**, p 517–536
24. L. Papeleux and J.P. Ponthot, Finite Element Simulation of Springback in Sheet Metal Forming, *J. Mater. Process. Technol.*, 2002, **125**, p 785–791
25. T. Buranathiti, J. Cao, W. Chen, W.L. Baghdasaryan, and Z.C. Xia, Approaches for Model Validation: Methodology and Illustration on a Sheet Metal Flanging Process, *J. Manuf. Sci. Eng.-Trans. ASME*, 2006, **128**, p 588–597
26. S.K. Panthi, N. Ramakrishnan, K.K. Pathak, and J.S. Chouhan, An Analysis of Springback in Sheet Metal Bending Using Finite Element Method (FEM), *J. Mater. Process. Technol.*, 2007, **186**, p 120–124
27. M. Firat, B. Kaftanoglu, and O. Eser, Sheet Metal Forming Analyses with an Emphasis on the Springback Deformation, *J. Mater. Process. Technol.*, 2008, **196**, p 135–148
28. S.L. Zang, C. Guo, S. Thuillier, and M.G. Lee, A Model of One-Surface Cyclic Plasticity and Its Application to Springback Prediction, *Int. J. Mech. Sci.*, 2011, **53**, p 425–435
29. H. Lim, M.G. Lee, J.H. Sung, and R.H. Wagoner, Time-Dependent Springback of Advanced High Strength Steels, *Int. J. Plast.*, 2012, **29**, p 42–59
30. S. Chatti and N. Hermi, The Effect of Non-linear Recovery on Springback Prediction, *Comput. Struct.*, 2011, **89**, p 1367–1377
31. P.A. Eggertsen and K. Mattiasson, On Constitutive Modeling for Springback Analysis, *Int. J. Mech. Sci.*, 2010, **52**, p 804–818
32. S. Bouvier, J.L. Alves, M.C. Oliveira, and L.F. Menezes, Modelling of Anisotropic Work-Hardening Behaviour of Metallic Materials Subjected to Strain-Path Changes, *Comput. Mater. Sci.*, 2005, **32**, p 301–315
33. R.K. Verma and A. Haldar, Effect of Normal Anisotropy on Springback, *J. Mater. Process. Technol.*, 2007, **190**, p 300–304
34. J.W. Lee, M.G. Lee, and F. Barlat, Finite Element Modeling Using Homogeneous Anisotropic Hardening and Application to Spring-Back Prediction, *Int. J. Plast.*, 2012, **29**, p 13–41
35. F. Yoshida and T. Uemori, A Model of Large-Strain Cyclic Plasticity Describing the Bauschinger Effect and Work Hardening Stagnation, *Int. J. Plast.*, 2002, **18**, p 61–686
36. F. Yoshida and T. Uemori, A Model of Large-Strain Cyclic Plasticity and Its Application to Springback Simulation, *Int. J. Mech. Sci.*, 2003, **45**, p 1687–1702